Research Article

Cancer Immunology Research

T-cell Responses in the Microenvironment of Primary Renal Cell Carcinoma—Implications for Adoptive Cell Therapy

Rikke Andersen[1,2], Marie Christine Wulff Westergaard[1], Julie Westerlin Kjeldsen[1], Anja Müller[3], Natasja Wulff Pedersen[4], Sine Reker Hadrup[4], Özcan Met[1,2], Barbara Seliger[3], Bjarne Kromann-Andersen[5], Thomas Hasselager[6], Marco Donia[1,2], and Inge Marie Svane[1,2]

Abstract

In vitro expansion of large numbers of highly potent tumor-reactive T cells appears a prerequisite for effective adoptive cell therapy (ACT) with autologous tumor-infiltrating lymphocytes (TIL) as shown in metastatic melanoma (MM). We therefore sought to determine whether renal cell carcinomas (RCC) are infiltrated with tumor-reactive T cells that could be efficiently employed for adoptive transfer immunotherapy. TILs and autologous tumor cell lines (TCL) were successfully generated from 22 (92%) and 17 (77%) of 24 consecutive primary RCC specimens and compared with those generated from metastatic melanoma. Immune recognition of autologous TCLs or fresh tumor digests was observed in $CD8^+$ TILs from 82% of patients (18/22). Cytotoxicity assays confirmed the tumoricidal capacity of RCC-TILs. The overall expansion capacity of RCC-TILs was similar to MM-TILs. However, the magnitude, polyfunctionality, and ability to expand in classical expansion protocols of $CD8^+$ T-cell responses was lower compared with MM-TILs. The RCC-TILs that did react to the tumor were functional, and antigen presentation and processing of RCC tumors was similar to MM-TILs. Direct recognition of tumors with cytokine-induced overexpression of human leukocyte antigen class II was observed from $CD4^+$ T cells (6/12; 50%). Thus, TILs from primary RCC specimens could be isolated, expanded, and could recognize tumors. However, immune responses of expanded $CD8^+$ RCC-TILs were typically weaker than MM-TILs and displayed a mono-/oligofunctional pattern. The ability to select, enrich, and expand tumor-reactive polyfunctional T cells may be critical in developing effective ACT with TILs for RCC. In summary, TILs isolated from primary RCC specimens could recognize tumors. However, their immune responses were weaker than MM-TILs and displayed a mono-/oligofunctional pattern. The ability to select and expand polyfunctional T cells may improve cell therapy for RCC. *Cancer Immunol Res; 6(2); 222–35. ©2018 AACR.*

Introduction

Adoptive cell therapy (ACT), based on the infusion of expanded autologous tumor-infiltrating lymphocytes (TIL), has demonstrated durable complete tumor regressions in metastatic melanoma (MM; refs. 1–8). TIL therapy relies on the infusion of potent TILs. In recent years, optimal phenotype, differentiation, and homing characteristics of TILs to achieve durable cancer regression were described (9). Nevertheless, the ability to recognize autologous tumor cells through their T-cell receptor (TCR) represents the essential characteristic of effective TILs.

Whereas tumor-reactive TILs can be generated from the majority of metastatic melanoma specimens (10, 11), the success rate appears lower for other cancers (12–16). Results from two recent studies (12, 14) indicated that the tumor microenvironment (TME) of renal cell carcinoma (RCC) harbors tumor-reactive T cells, but how the magnitude and functional quality of these immune responses compare with other tumor types is unknown. Previous clinical trials investigating TIL therapy for RCC have shown modest success (17); however, none of these early trials used current TIL expansion methods and preparative chemotherapy regimens, opening the possibility to revisit TIL therapy for RCC. Consistent durable objective responses achieved in small numbers of patients treated with cytokine-based immunotherapy (18) or checkpoint inhibitors (19) demonstrate that immunologic control of RCC can be feasible.

These observations prompted us (i) to characterize the immune responses of TILs generated from primary RCC tumors (RCC) from 24 patients and (ii) to compare RCC-TILs

[1]Center for Cancer Immune Therapy, Department of Hematology, Herlev Hospital, University of Copenhagen, Herlev, Denmark. [2]Department of Oncology, Herlev Hospital, University of Copenhagen, Herlev, Denmark. [3]Institute of Medical Immunology, Martin Luther University Halle-Wittenberg, Halle, Germany. [4]Division for Immunology and Vaccinology, Technical University of Denmark, Lyngby, Denmark. [5]Department of Urology, Herlev Hospital, University of Copenhagen, Herlev, Denmark. [6]Department of Pathology, Herlev Hospital, University of Copenhagen, Herlev, Denmark.

Note: Supplementary data for this article are available at Cancer Immunology Research Online (http://cancerimmunolres.aacrjournals.org/).

M. Donia and I.M. Svane contributed equally to this article.

Corresponding Authors: Inge Marie Svane, Copenhagen University Hospital, Herlev Ringvej 75, Herlev 2730, Denmark. Phone: 453-868-2131; Fax: 453-868-3457; E-mail: inge.marie.svane@regionh.dk; and Marco Donia, marco.donia@regionh.dk

doi: 10.1158/2326-6066.CIR-17-0467

AACR

to MM-TILs. T-cell responses were detected in the majority of RCCs analyzed. Extensive characterization of TILs revealed a unique functional pattern, with weaker and mostly mono- or oligofunctional $CD8^+$ T-cell responses compared with metastatic melanoma. These findings have relevance for the development of ACT for patients with RCC.

Materials and Methods

Patients and samples

Twenty-four patients with histologically confirmed RCC, undergoing radical or partial nephrectomy at the Department of Urology, Herlev Hospital (Herlev, Denmark) in the period from October 2013 to November 2015, were enrolled in the study. The study was approved by the Ethics Committee of the Capital region of Denmark and the Danish Data Protection Agency. All patients signed a written consent form. Tumor specimens of at least 1 cm^3 were obtained from different sites of the primary RCC tumor to account for intratumor heterogeneity (20). Blood samples were collected prior to surgery; peripheral blood mononuclear cells (PBMC) were isolated with standard methods and cryopreserved at −140°C until use.

Treatment with autologous TILs resulted in high rates of tumor regression in metastatic melanoma (1). To compare the phenotype and functionality of RCC-TILs to a reference tumor histology, we used TILs and matched autologous tumor cell lines (TCL) derived from tumor specimens of patients with American Joint Committee on Cancer stage IV melanoma enrolled in one of the following clinical trials [ClinicalTrials.gov identifier: NCT00937625 (8); NCT02278887, recruiting; NCT02379195, recruiting]. TILs and TCLs from metastatic melanoma were established and analyzed in parallel to RCC specimens. Because of the limited availability of TILs from metastatic melanoma (most were typically used for clinical application), most MM-TIL samples could not be used for all comparison analyses with RCC-TILs. Rather, different individual MM-TILs were randomly selected for single comparison analyses. All analyses were performed once for each patient. One additional cohort of RCC-TILs ($n = 6$) obtained from primary clear cell RCC tumors from the University of Halle (Halle, Germany) was shipped to Herlev Hospital and cultured as described below and used for additional phenotypic characterization analyses (expression of PD-1, LAG-3, TIM-3, and CD57), as described below.

Generation of young TIL cultures

Freshly resected tumor specimens were immediately transported to the laboratory in RPMI1640 (Thermo Fisher Scientific)–based transport media and cut into 1 to 3 mm^3 fragments that were used for generation of TILs, fresh tumor digests (FTD) or TCL. Forty-eight tumor fragments were used for TIL generation and placed in individual wells of 24-well culture plates (Nunc) with 2 mL complete medium (CM) consisting of 90% RPMI1640 (Thermo Fisher Scientific), 10% heat-inactivated AB Human Serum (HS; Sigma-Aldrich), 6,000 IU/mL IL2 (Proleukin, Novartis), penicillin/streptomycin, and fungizone (Bristol-Myers Squibb) as described previously (21). The plates were placed in a humidified 37°C incubator with 5% CO_2. Half of the medium was replaced at day 5 and thereafter three times per week. TIL cultures were expanded *in vitro* directly from the tumor fragments according to the "minimally expanded" or "young TIL (Y-TIL) method," by pooling TIL microcultures derived from separate tumor fragments, as described previously (21). Y-TIL cultures were considered established if one pooled bulk TIL culture of $>100 \times 10^6$ cells was obtained within 60 days from surgery.

Rapid expansion protocol

To further test the expansion capacity of Y-TILs for clinical application, massive expansion in a standard 14-day rapid expansion protocol (REP) was performed on cryopreserved or freshly generated Y-TILs. REPs were performed in duplicates and in smaller scale than for patient treatment (test REPs), but otherwise exactly as for clinical application, as described previously (21). Y-TILs were thawed and rested in CM for 2 days prior to initiating the REP. A total of 1×10^5 Y-TILs (in duplicates) were expanded in a small-scale REP using 30 ng/mL anti-CD3 antibodies (OKT3, from Janssen-Cilag or Miltenyi Biotec), irradiated (40 Gy) allogeneic feeder cells (PBMCs from at least three different healthy donors) in a ratio of 1:200 in medium containing 6,000 IU/mL IL2. The cells were incubated upright in 25-cm^2 tissue culture flasks at 37°C in 5% CO_2 (21). Cell concentration was determined on days 7, 9, 12, and 14, and cells were split into larger flasks and additional media added as needed to maintain cell densities around $1–2 \times 10^6$ cells/mL. The cells were harvested on day 14 and fold expansion calculated. Y-TILs expanded in the REP are referred to as REP-TILs in this article.

REPs in very small scale (mini-REPs) with alternative cytokine combinations were performed in single wells in 96-well plates. Briefly, 5×10^3 Y-TILs (in duplicates) were rapidly expanded as described above, using IL2 alone (6,000 IU/mL) or different combinations of IL2 (6,000 IU/mL), IL7 (100 ng/mL), IL15 (100 ng/mL), and IL21 (100 ng/mL). Cytokines were added on day 0 and every time medium was replaced (on day 5 and thereafter approximately every other day). RCC-Y-TILs used were elected for their high reactivity but low or absent reactivity after classical REP. The six RCC-Y-TILs used were RCC4, RCC6, RCC12, RCC19, RCC23, and RCC26. One initial screening of seven different cytokine combinations was made in three RCC-Y-TILs. The following cytokine cocktails were used: IL2; IL15 + IL2; IL7 + IL15 + IL21; IL2 + IL21; IL2 + IL7 + IL21; IL2 + IL7; IL15 + IL21. We next performed mini-REPs in three additional patients with only the three cytokine combinations where we detected responses after REP in the first screening: IL2 alone, IL7 + IL15 + IL21, and IL15 + IL21.

Autologous FTDs and TCLs

Single-cell suspensions were obtained from tumor fragments after overnight digestion. Briefly, after overnight incubation with enzyme cocktails (containing 1 mg/mL collagenase type IV, Sigma-Aldrich, and 0.0125 mg/mL dornase alpha, Pulmozyme, Roche), the obtained single-cell suspensions were passed through 70-μm strainers and immediately cryopreserved. The cellular composition of the resulting single-cell suspensions, which contained uncultured tumor cells and was named FTDs, was not further analyzed. For analysis of TIL reactivity against FTDs, the single-cell suspensions were thawed and used immediately after a trypan blue viability count.

Autologous short-term (<10 *in vitro* passages) cultured RCC and metastatic melanoma TCLs were generated from fresh tumor fragments or from cells recovered from the transport media, as described previously (11). Briefly, TCLs were

established using standard splitting methods of cancer-like growing adherent cells in R10 media (containing RPMI1640 with 10% FBS supplemented with 500 ng/mL Solu-Cortef). All autologous TCLs were established at our laboratory and initially identified from their morphology and *in vitro* growth patterns. Additional validation of RCC-TCLs was carried out following cytospin centrifugation of freshly detached RCC cell lines. A combination of morphologic evaluation (according to standard cytologic criteria of malignancy (22) and IHC staining of formalin-fixed, paraffin-embedded tissue for various RCC markers was used. Supplementary Figure S1 shows a representative image from a representative patient (RCC12). In a few cases, where the morphology or growth pattern of MM-TCLs was not typical of adherent tumor cell lines, the melanocyte lineage was confirmed with PCR for melanocyte antigens, as described previously (11). TCLs were not otherwise authenticated or tested for mycoplasma infection. The *in vitro* growth of RCC-TCLs was not always sufficient to carry out all experiments described below, but in all cases, these experiments were conducted with at least 12 of 17 RCC-TCLs generated in this study.

Flow cytometry: antibodies and stainings

For phenotype analysis of *in vitro* expanded TILs, the cells were stained at 4°C for 30 minutes in PBS (Lonza), washed and resuspended in PBS, and immediately analyzed. The following antibodies were used: CD3-AmCyan, CD4-PerCP, CD45RO-PE, CD45RA-APC, CD57-FITC, CD27-PE, CD62L-APCCy7, CD56-PeCy7, CD56-PE (all from BD Biosciences), CD8-PB (Dako), CCR7-FITC (R&D Systems), CD28-APC (Beckman Coulter). 7-aminoactinomycin D (7-AAD, BD Biosciences) was added as control in a separate tube, to evaluate the amount of dead cells. At least 50,000 TILs were acquired with a FACS Canto II (BD Biosciences).

For functional characterization and phenotype analysis of tumor-reactive cells, the following antibodies were used: CD3-FITC, CD4-PerCP, or CD4-Qdot705 (Thermo Fisher Scientific), CD8-Qdot605 (Thermo Fisher Scientific), CD107a-Brilliant Violet 421, (TNF) TNF-APC, (IFNγ) IFNγ-PeCy7, PD-1-PE (eBioscience), LAG-3-FITC (Thermo Fisher Scientific), TIM-3-Qdot 655, and CD57-PECF594. The Live/Dead Fixable Near-IR Dead Cell Stain (Thermo Fisher Scientific) was used to discriminate dead cells. Where not indicated, antibodies were obtained from BD Biosciences.

Functional characterization of TILs

In vitro expanded TILs and/or PBMCs were tested for reactivity against autologous short-term cultured TCLs (TILs and PBMCs) or autologous FTDs (only TILs) in coculture assays as described previously (8, 11). *In vitro* expanded TILs and/or PBMCs were tested for reactivity against autologous short-term cultured TCLs (TILs and PBMCs) or autologous FTDs (only TILs) in coculture assays, as described previously (8, 11). Briefly, TILs and PBMCs were thawed and rested overnight in RPMI1640 + 10% HS, thereafter washed twice and cocultured for 5 hours at 37°C with 5% CO_2 in the air with autologous FTDs (thawed and washed twice) or autologous short-term cultured TCLs, pretreated with 100 IU/mL (IFNγ; Imukin, Boehringer-Ingelheim) for 72 hours or left untreated at an effector/target (E/T) ratio of 3:1 to 6:1. Anti-CD107a antibodies and GolgiPlug (BD Biosciences, dilution of 1:1,000) were added at the beginning of the incubation. Parallel cultures without cancer cells served as unstimulated control. Positive control wells were set up with the addition of *Staphylococcus* enterotoxin B (SEB 5 μg/mL, Sigma-Aldrich) in selected experiments. After 5 hours, the cells were washed twice with PBS and stained with antibodies directed to surface markers and live/dead reagents. Cells were washed one more time, fixed overnight, permeabilized (using the Foxp3/Transcription Factor Staining Buffer set, eBioscience), and subsequently stained with antibodies for intracellular cytokines.

In selected experiments, a functional analysis was combined with phenotype markers to assess the differentiation and dysfunctional state of tumor-reactive TILs. Because IFNγ production was not observed frequently in RCC-TILs (see Results), and we generally observed quite high TNF production in unstimulated samples (TILs without tumor), in these experiments, we gated on $CD8^+CD107a^+$ tumor-reactive T cells to analyze the phenotype of tumor-reactive TILs. On the basis of these observations, CD107a upregulation might indeed be a more reliable marker for T-cell reactivity to RCC especially in TIL populations with small responses. At least 50,000 (basic functional characterization) or 500,000 live TILs (phenotype of tumor-reactive TILs) were acquired, respectively, with a BD FACS Canto II or a BD LSRII.

Tumor reactivity was evaluated by assessing the amount of live $CD4^+$ or $CD8^+$ T cells expressing at least one of the following T-cell functions: TNF, IFNγ, or CD107a (LAMP-1). These three functions were chosen on the basis of previous data with metastatic melanoma–reactive TILs, which expressed at least one of these three functions in >90% of cases (11). A specific antitumor response was defined as the detection of responses larger than twice the background (i.e., unstimulated samples) with a minimum number of 50 positive events and at least a difference of 0.5% from the background. The frequency of tumor-reactive cells in stimulated samples was subtracted from unstimulated samples. The limit of significance was 0.5%.

Cytotoxicity assay

The cytotoxic activity of TILs was tested with a standard chromium 51 (^{51}Cr) release assay, as described elsewhere (23). In brief, 5×10^3 ^{51}Cr-labeled autologous tumor cells (TCL) in duplicates were cocultured with TILs at 37°C for 4 hours (maximum E/T ratio of 90:1 and titrated) in RPMI1640 + 10% HS. Thereafter, ^{51}Cr-release was measured and percentage tumor lysis was calculated using the following formula: [(experimental release − spontaneous release)/(maximum release − spontaneous release)] × 100. In selected assays, lysis was blocked using anti-HLA class I (W6/32, BioLegend) antibodies, 20 μg/mL.

Enrichment of tumor-reactive T cells

Y-TILs were thawed and rested for 48 hours in RPMI1640 + 10% HS. For autologous tumor cell stimulation, TILs were cocultured for 5 hours with autologous TCLs at an E/T ratio of 3:1. Anti-CD107a antibodies (conjugated with PE or BV421, two different clones, obtained, respectively, from Diaclone and from BD Biosciences) were added before incubation. After 5 hours of incubation, cells were washed twice with PBS and stained with CD3 and CD8 antibodies and sorted by FACS using the BD FACSAria cell sorter. Sorted $CD8^+CD107a^+$ cells were further expanded 10 + 10 days in two sequential mini/test-REPs (adjusted for the sorted cell numbers) and

antitumor responses tested in coculture assay with autologous TCLs (as described above).

RNA extraction and PCR analysis of HLA class I APM components

Eleven RCC-TCLs and 16 MM-TCLs were used for these analyses. All the RCCs and MM-TCLs were generated and validated in our laboratory as described above, except for two of the RCC-TCLs included in these analyses (Caki-1 and Caki-2), which were obtained directly from ATCC and passaged for less than 10 times. Total cellular RNA from 1–5 $\times$ 10^5 cells/sample was extracted and subjected to qPCR analysis as described recently (24). The specific primer sequences and PCR conditions are provided in Supplementary Table S1. Briefly, *in vitro* transcription was performed with 500 ng RNA/sample using the RevertAid H minus First-Strand cDNA Synthesis Kit according to the supplier's suggestions (Fermentas) prior to PCR employing respective primers (Supplementary Table S1) and the Platinum SYBR Green qPCR SuperMix-UDG (Invitrogen) for amplification using 40 cycles, 90°C, 15 seconds, 58–60°C annealing temperature, 30 seconds. Relative mRNA expression levels were calculated with the ΔC_t method and normalized to β-actin.

Analysis of HLA and PD-L1 expression on tumor cells

Semiquantitative expression of HLA class I and II antigens on TCLs from RCC and metastatic melanoma were assessed by staining the freshly detached cancer cells with anti HLA-ABC or HLA-DP, DR, DQ antibodies, or relevant isotype controls. Autologous TCLs were pretreated with 100 IU/mL IFNγ for 72 hours or were left untreated. The tumor cells were detached, divided in FACS tubes, washed, stained with surface antibodies (only one antibody for each FACS tube), and 2 μL 7-AAD was added to each sample 5 minutes before acquisition. To more easily compare the relative marker expression of different TCLs, voltage parameters were adjusted for each isotype-stained TCL to achieve similar mean fluorescence intensities (MFI) in all samples. TCLs were identified as positive for HLA class II when the MFI of the studied antibody sample exceeded at least three times the isotype control stained and positive for PD-L1 when the MFI of the studied antibody sample exceeded at least twice the isotype control stained.

Flow cytometry data processing and statistical analysis

For functional and phenotypic characterization analyses of tumor-reactive cells, data were initially analyzed in FlowJo 9.7.1 with Boolean combination gates. For functional characterization, Boolean combination gates were made for the three functional markers (CD107a, IFNγ, and TNF), generating seven gates each showing the percentage of $CD8^+$ cells expressing a unique combination of the three markers. For phenotypic characterization of tumor-reactive TILs, live $CD8^+$ T cells were gated on $CD107a^+$, and Boolean combination gates were made for the four surface markers (PD-1, LAG-3, TIM-3, and CD57) resulting in 16 individual gates, each showing the percentage of $CD8^+CD107a^+$ cells expressing a unique combination of the four markers. TILs from the additional RCC cohort were analyzed for expression of the four surface makers in the exact same way, but not gated on $CD107a^+$. Data were exported into Pestle 1.7 (courtesy of Dr. Roederer, Immunotechnology Section, VRC/NIAID/NIH, Bethesda, MD), formatted, and the background was subtracted. Analysis and presentation of distributions was performed using Simplified Presentation of Incredibly Complex Evaluations (SPICE) 5.35, downloaded from http://exon.niaid.nih.gov (25). In SPICE, thresholds were set at 0.1 for functional characterization analysis and 0.01 for phenotypic analysis of tumor-reactive cells. Comparison of bar charts and pie charts was performed using Wilcoxon signed rank test and a partial permutation test, respectively, as described previously (25). Other analyses were carried out with Excel 2010 or GraphPad Prism 5. The magnitude of tumor responses and HLA class I antigen expression in RCC and metastatic melanoma were compared with two-tailed Mann-Whitney *U* test. The frequency of patients with T-cell responses in RCC and metastatic melanoma was compared with Fisher exact test. IFNγ-treated or untreated samples and mini-REPs with alternative cytokines in RCC were compared using paired Wilcoxon signed rank nonparametric tests. In all analyses, a two-sided *P* value of <0.05 was considered statistically significant, and all *P* values were presented without adjustment for multiple comparisons.

Results

Expansion and phenotype of TILs

Y-TIL cultures were established from 22 of 24 (92%) primary RCC specimens. Patient and tumor characteristics are summarized in Supplementary Table S2. Median days in culture of Y-TILs were 28 days (range, 14–60) and median number of TILs recovered was 177 $\times$ 10^6 (range, 100–336 $\times$ 10^6). Establishment of Y-TILs in metastatic melanoma was successful in all cases (17/17 samples), generally faster than RCC (median days in culture 20 days; range, 13–60, $P = 0.047$ vs. RCC-Y-TILs) and with similar amount of cells recovered (median 190 $\times$ 10^6; range, 35–352 $\times$ 10^6, $P = 0.52$ vs. RCC-Y-TILs).

The phenotypic characteristics of Y-TILs from both RCC and metastatic melanoma are shown in Fig. 1. Y-TILs consisted mainly of $CD3^+$ lymphocytes (87.7% vs. 89.4%; $P = 0.79$), with fewer $CD3^-CD56^+$ natural killer (NK) cells (9.6% vs. 8.2%; $P = 0.9$). RCC-Y-TILs contained less $CD8^+$ T cells compared with MM-Y-TILs (25.2% vs. 48.5%; $P = 0.007$) and showed a higher CD4/CD8 ratio in RCC (2.1 vs. 0.8; $P = 0.02$, Fig. 1A). A detailed analysis of the relative distribution of lymphocyte subpopulations in individual RCC-Y-TILs is shown in Supplementary Table S3, where the extent of variation between individual patients can be appreciated. $CD4^+$ and $CD8^+$ Y-TILs from both from RCC and metastatic melanoma consisted almost exclusively of effector memory cells (T_{EM}: $CD45RO^+$, $CD45RA^-$, $CCR7^-$), with similar median percentages of $CD8^+$ T_{EM} (95.5% vs. 95%, Fig. 1B) but higher percentage of $CD4^+$ T_{EM} in RCC (98% vs. 95%, $P = 0.047$; Fig. 1C). The expression of CD28, CD56, and CD57 on $CD8^+$ Y-TILs appeared similar in both tumor types with broad variations among patients (Fig. 1B). However, $CD8^+$ and $CD4^+$ MM-Y-TILs expressed more CD27 ($CD8^+$ and $CD4^+$, $P < 0.01$) and CD62L ($CD8^+$, $P = 0.01$; $CD4^+$, $P < 0.01$; Fig. 1B and C). $CD4^+$ MM-Y-TIL expressed more CD57 ($P = 0.01$; Fig. 1C).

All 22 RCC-Y-TILs were further expanded in small-scale REPs. TILs expanded a median of 1,693-fold (range, 530–4,395; Supplementary Table S2), which was similar to MM-TILs (Fig. 1D, only 14 RCC were tested in parallel with 11 metastatic melanoma). Retrospectively, we found that randomly selected Y-TILs

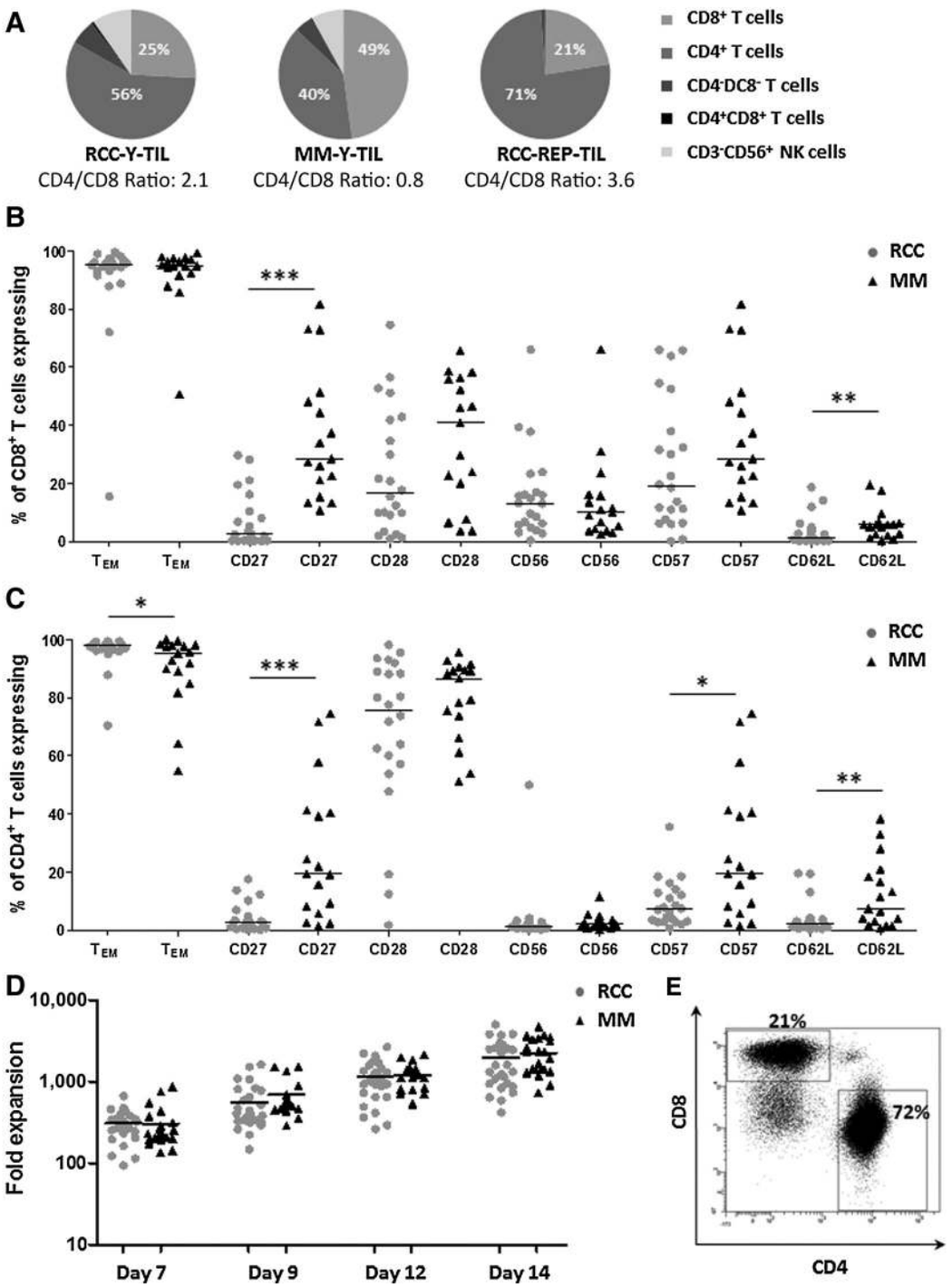

Figure 1.

Phenotypic characterization of Y-TILs and REP. **A–C,** The figures show the phenotype of *in vitro* expanded Y-TILs from 22 RCC and 17 metastatic melanoma specimens. **A,** The pie charts illustrate the phenotype characteristics of all RCC and metastatic melanoma patients analyzed. Median values of the proportion of TILs expressing the following surface markers are shown: $CD3^+CD8^+$, $CD3^+CD4^+$, $CD3^+CD4^+CD8^+$, $CD3^+CD4^-CD8^-$, and $CD3^-CD56^+$). RCC-Y-TILs contained less $CD8^+$ T cells ($P = 0.007$) and more $CD4^+$ T cells than MM-Y-TILs; however, this difference was not statistically significant ($P = 0.09$). **B** and **C,** Dot plots show the proportion of Y-TILs expressing the depicted phenotypic markers on $CD8^+$ (**B**) and $CD4^+$ T cells (**C**) in RCC ($n = 22$, gray dots) and metastatic melanoma ($n = 17$, black triangles). T_{EM}, T effector memory ($CD45RO^+$, $CD45RA^-$, $CCR7^-$). Lines show median values. *, $P < 0.05$; **, $P \leq 0.01$; ***, $P \leq 0.001$. **D,** To directly compare the expansion capacity in RCC and metastatic melanoma, small-scale REPs in 14 randomly selected RCC samples (performed in duplicates) were carried out in parallel with 11 metastatic melanoma samples (performed in duplicates). The fold expansion of TILs during REP was similar in RCC (gray dots) and metastatic melanoma (black triangles): median fold expansion on day 7 ($P = 0.17$), day 9 ($P = 0.08$), day 12 ($P = 0.7$), or on day 14 ($P = 0.3$). Lines show median values. **E,** The FACS plots illustrate the proportion of $CD3^+$ TILs staining positive for CD4 and CD8 from a representative patient (RCC16).

used for comparison of REP expansions were established faster in metastatic melanoma (median days in culture 17; range, 13–37) compared with RCC (median days in culture 28; range, 18–60; $P = 0.018$).

As expected, NK cells did not expand during the REP and disappeared from all REP cultures (Fig. 1A; Supplementary Table S2). In most cases, the CD4/CD8 ratio in RCC increased after REP, from median 2.1 (range, 0.3–12.7) in Y-TILs to median 3.6 (range, 0.5–56.1; $P = 0.02$).

In conclusion, these observations suggested that some fundamental characteristics of TILs are similar between RCC- and MM-TILs (percentage of T cells and of T_{EM}, expansion, large variation between individual patients). However, other characteristics (CD4/CD8 ratio, expression of CD27 and CD62L on $CD8^+$ and $CD4^+$ TILs, and expression of CD57 on $CD4^+$ TILs) appeared different; however, because the time in culture of MM-Y-TILs was shorter than RCC-Y-TILs (20 days vs. 28 days, see above), we cannot exclude that these differences are due to changes induced by prolonged *in vitro* culturing.

Tumor-reactive $CD8^+$ TILs

We next investigated the ability of TILs to recognize autologous tumor antigens. Short-term cultured autologous TCLs, serving as a source of naturally presented autologous tumor antigens, were generated from 17 of 22 (77%) RCCs. Single-cell suspensions obtained from FTD were available for all RCCs.

Immune recognition of RCC-TCLs by $CD8^+$ Y-TILs was observed in 12 of 17 patients (71%) and by $CD8^+$ REP-TILs in 7 of 17 patients (35%; Fig. 2). In metastatic melanoma, $CD8^+$ Y-TIL responses to autologous TCLs were detected in all but one of the 14 Y-TILs analyzed (93%, $P = 0.18$ vs. RCC). The magnitude of $CD8^+$ T-cell responses was weaker in RCC (in TILs with responses, 2.2% vs. 10.8% in metastatic melanoma; $P = 0.0001$), as shown in Fig. 2A. $CD8^+$ T-cell responses against autologous FTDs were detected in 15 of 22 RCC-Y-TILs (68%) and 13 of 22 REP-TIL cultures (59%; Fig. 2C and D). Although not identical, both the frequency and magnitude of $CD8^+$ responses against FTDs reflected those observed against short-term cultured TCLs. Overall, $CD8^+$ T-cell responses against autologous tumor antigens (either presented in TCLs or in FTDs) were detected in 17 of 22 RCC-Y-TILs (77%) and 14 of 22 RCC-REP-TILs (64%). One patient (RCC10) had a very low response detected in REP-TILs only; thus, the total number of patients with tumor-reactive $CD8^+$ TILs was 18 of 22 (82%; Fig. 2C and D). Cytokine production (TNF and IFNγ) and CD107a mobilization in $CD8^+$ RCC-Y-TILs after coculture with autologous TCLs are shown in 2 representative patients in Fig. 2E and F. Supplementary Table S4 shows a summary of tumor reactivity and HLA expression on RCC TCLs in individual patients. We found that TILs that contained tumor-reactive $CD8^+$ T cells had spent shorter time in culture compared with TILs without tumor-reactive $CD8^+$ T cells ($P = 0.02$). This may be due to heavier T-cell infiltration, or alternatively due to a higher proliferation capacity of TILs from patient samples with tumor reactivity.

We and others have reported detectable but low magnitude T-cell responses directed to autologous metastatic melanoma antigens in the PBMCs of patients before treatment with immunotherapy (8, 26). By screening the peripheral blood of 6 patients with RCC in cocultures with TCLs (PBMCs from 5 patients with detectable tumor reactivity in Y-TILs were used), we did not detect responses over the limit of detection used in this study (0.5% of either $CD4^+$ or $CD8^+$ T cells, as shown in Supplementary Fig. S2). Thus, tumor-reactive $CD8^+$ T cells were enriched in the TME.

Changes in TIL reactivity during massive expansion

Effective TIL therapy relies on *in vitro* generation of potent tumor-reactive TILs in numbers sufficient for clinical application. This prompted us to determine whether large quantities of tumor-reactive TILs could be expanded massively with current protocols used for TIL expansion (REP). In both TILs from RCC and metastatic melanoma, we observed an overall reduced reactivity following REP compared with minimally expanded TILs (Y-TILs; Supplementary Fig. S3A; Fig. 3C and D). In 5 of 12 RCC-TILs, reactivity was lost, whereas in 11 MM-TILs, tumor reactivity was never lost completely (Supplementary Fig. S3B). The proportion of tumor-reactive $CD8^+$ TILs following REP appeared to drop to a larger extent in RCC-TILs compared with MM-TILs, as seen from Supplementary Fig. S3B. Nonetheless, these analyses could be biased by the low frequencies of tumor-reactive cells in RCC-Y-TILs, which in many cases are close to the detection limit; thus, a small drop might have resulted in undetectable responses. We conducted additional attempts to isolate $CD8^+$ tumor-reactive T cells from RCC- and MM-Y-TILs (TILs from 2 patients for each diagnosis) by electronic sorting of tumor-reactive cells ($CD107a^+$) and REP the sorted cells. Similar approaches were previously conducted with success in metastatic melanoma (27). Despite repeated attempts, we could not generate TILs enriched with tumor-reactive $CD8^+$ T cells from RCC-TILs, but the same approach was successful with MM-TILs in 2 of 2 cases (Supplementary Fig. S4). Because previous studies have shown that the use of cytokines other than IL2 during the REP, such as IL21, IL15, and IL7, can support the expansion of exhausted T cells (27, 28), we tested whether combinations of IL21, IL15, and IL7 could support expansion of tumor-reactive $CD8^+$ TILs in selected RCC-Y-TILs. We observed no difference in the magnitude of tumor reactivity (Supplementary Fig. S5) after mini-REPs with alternative cytokine combinations versus classical REP.

To verify the cytotoxic potential of TILs, samples from five representative RCCs with detectable $CD8^+$ T-cell responses against autologous TCLs were tested in cytotoxicity assays. Cytotoxicity was detected but was typically low and further reduced after REP. In selected experiments, HLA class I blockade was tested and almost abrogated cytotoxicity (Supplementary Fig. S6).

Polyfunctional characterization of tumor-reactive $CD8^+$ T cells

Polyfunctionality is a desirable feature of potent $CD8^+$ T cells, well known in infections (29), but only recently described in cancer immunity (11, 30). This feature is known to correlate with antigen sensitivity and TCR affinity for cognate antigen (31, 32), antigen concentration (33), and, partially, differentiation status (34). We recently showed that polyfunctional T cells dominate the periphery after successful TIL therapy for cancer (35). Thus, we characterized the functional patterns of tumor-reactive $CD8^+$ T cells. Tumor-reactive $CD8^+$ RCC-Y-TILs were less polyfunctional compared with corresponding MM-Y-TILs, with the majority (>70%) of tumor-reactive $CD8^+$ RCC-Y-TILs generating only one T-cell function (monofunctional

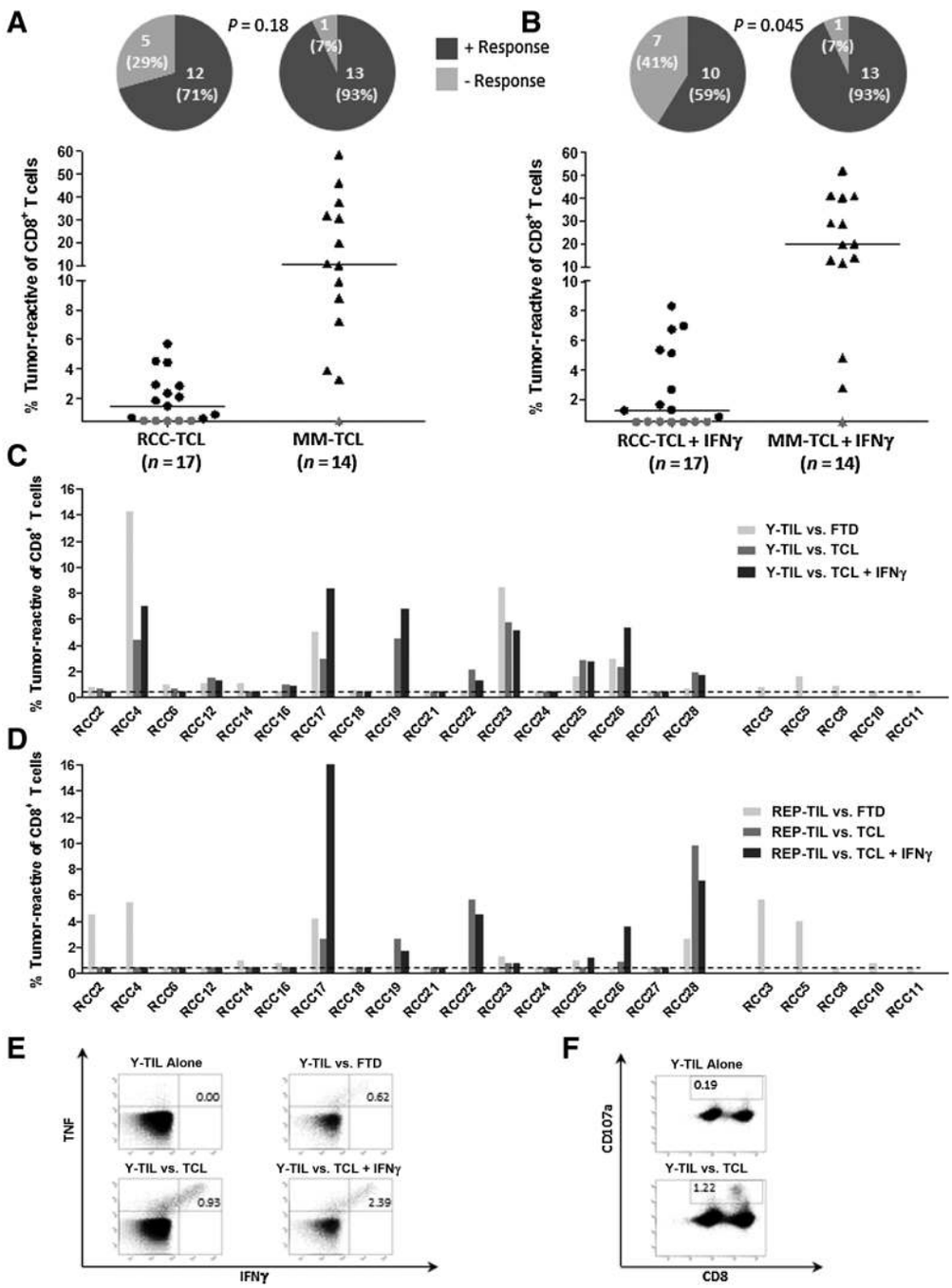

Figure 2.

CD8$^+$ T-cell responses in RCC and metastatic melanoma. The figure shows antitumor CD8$^+$ T-cell responses in RCC- ($n = 17$) and MM- ($n = 14$) Y-TILs and REP-TILs after coculture with autologous FTD or TCLs, treated with IFNγ (TCL + IFNγ) or left untreated (TCL), as described in Materials and Methods. Tumor-reactive T cells are defined as T cells expressing at least one of the following T-cell functions: TNF, IFNγ, or CD107a. **A** and **B,** Top, the number/(%) of patients containing Y-TILs with (dark gray) or without (light gray) CD8$^+$ T-cell responses against TCLs ± IFNγ is shown in the pie charts. No significant difference was found when comparing CD8$^+$ T-cell responses in Y-TILs cocultured with untreated TCLs from RCC and metastatic melanoma ($P = 0.18$), whereas a higher percentage of MM-TILs had CD8$^+$ T-cell responses toward TCLs + IFNγ ($P = 0.045$). Bottom, dots and triangles represent RCC- and MM-TILs, respectively; black and gray symbols represent Y-TILs with or without CD8$^+$ responses against TCLs ± IFNγ, respectively. Limit of detection was 0.5%. Lines show median values. The magnitude of CD8$^+$ T-cell responses in Y-TILs against autologous TCLs (both untreated and treated with IFNγ) were lower in RCC compared with metastatic melanoma (when only TILs with responses are compared: untreated TCLs $P = 0.0001$; TCLs + IFNγ, $P = 0.0007$). **C** and **D,** The percentages of tumor-reactive CD8$^+$ Y-TILs (**C**) and CD8$^+$ REP-TILs (**D**) after coculture with autologous FTDs (light gray bars), untreated TCLs (dark gray bars), or TCLs + IFNγ (black bars) in individual RCC patients are shown. In patients where autologous TCLs were not available, TILs were only tested against FTDs (RCC3, RCC5, RCC8, RCC10, and RCC11). Dotted line, limit of detection (0.5%). **E** and **F,** The FACS plots demonstrate cytokine production (**E**; TNF and IFNγ) and CD107a mobilization in CD8$^+$ RCC-Y-TILs (**F**) after coculture with autologous tumor cells in two representative patients (RCC26 in **E** and RCC12 in **F**).

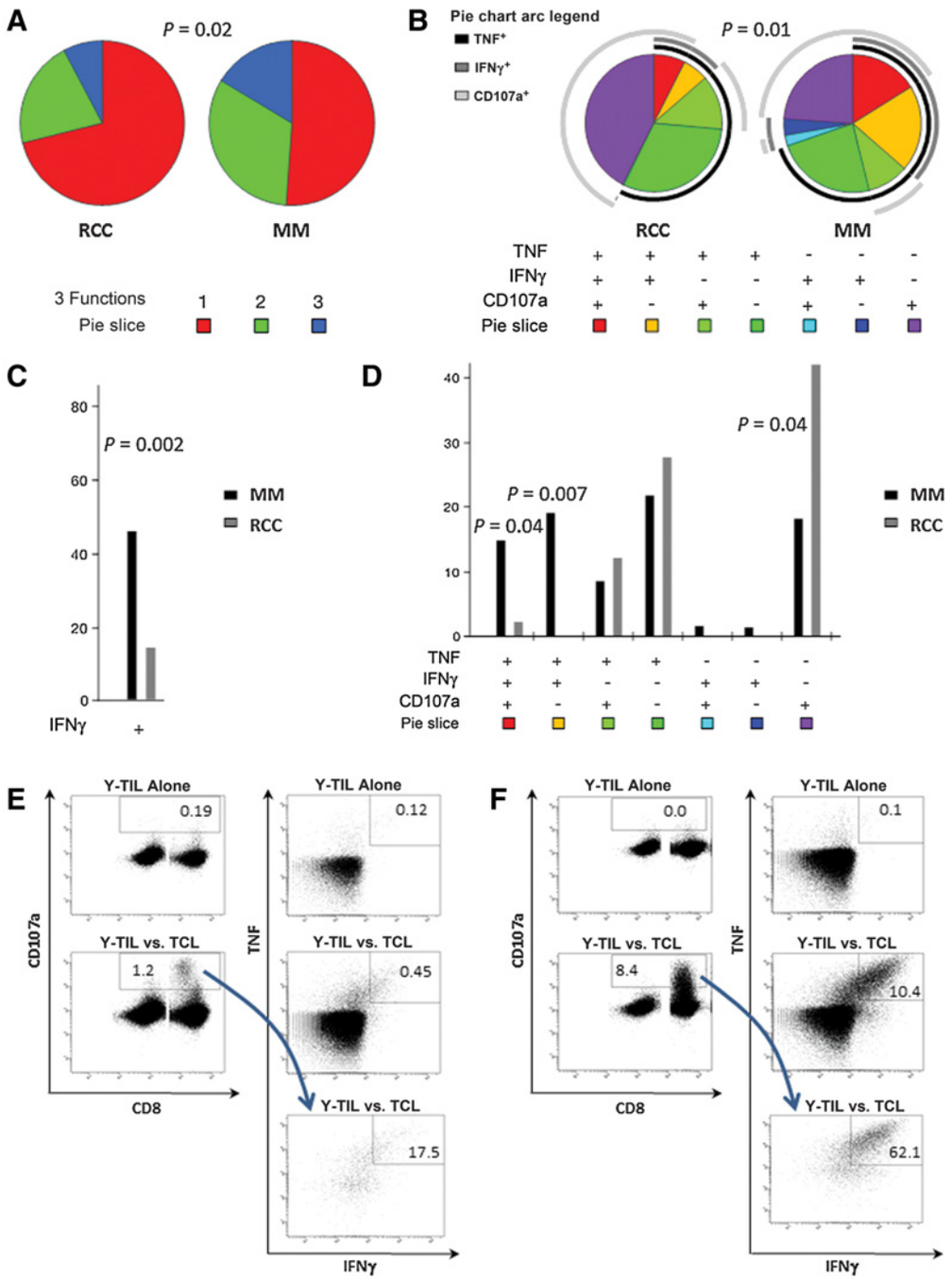

Figure 3.

Polyfunctional characterization of CD8$^+$ tumor-reactive T cells. The figure shows a graphical presentation of SPICE data analyses. CD8$^+$ Y-TIL subpopulations from RCC ($n = 12$) and metastatic melanoma ($n = 13$) were gated on cells expressing at least one of the three T-cell functions analyzed (IFNγ, TNF, and CD107a), and pie charts and columns illustrate the median values. **A,** The pie charts show the proportion of tumor-reactive CD8$^+$ T cells generating 1, 2, or 3 of the three T-cell functions analyzed, in RCC and metastatic melanoma, respectively. Tumor-reactive CD8$^+$ T cells in RCC-Y-TILs were less polyfunctional than metastatic melanoma ($P = 0.02$). **B** and **C,** The pie charts (**B**) and bar chart (**C**) illustrate the relative distribution of the seven combinations of the three T-cell functions generated by tumor-reactive CD8$^+$ T cells in RCC (gray bars) and metastatic melanoma (black bars), respectively. **B,** Tumor-reactive CD8$^+$ T cells in RCC-Y-TILs appeared less polyfunctional compared with metastatic melanoma ($P = 0.01$, permutation test), and a larger fraction of T cells mobilized CD107a without the production of cytokines (**B** and **C**; $P = 0.04$, vs. metastatic melanoma, corresponding to the purple pie slice). **D,** The bar chart shows that a smaller fraction of tumor-reactive CD8$^+$ T cells in RCC-Y-TILs produced IFNγ compared with metastatic melanoma ($P = 0.002$), indicating that IFNγ was most typically produced by MM-TILs. **E** and **F,** The FACS plots demonstrate CD107a mobilization and cytokine production (TNF and IFNγ) from CD8$^+$ RCC-Y-TILs after coculture with autologous tumor cells in a representative RCC patient (**E**; RCC12) and a representative melanoma patient (**F**). **E** and **F,** Only 17.5% of CD8$^+$CD107a$^+$ RCC-Y-TILs also produce cytokines (**E**), whereas 62.1% of CD8$^+$CD107a$^+$ RCC-Y-TILs also produce cytokines (**F**).

$CD8^+$ T cells) upon recognition of naturally presented autologous tumor antigens, in contrast to around 50% in metastatic melanoma ($P = 0.02$; Fig. 3A). The pie charts in Fig. 3B illustrate the relative distribution of TNF, IFNγ, and CD107a for RCC- and metastatic melanoma–reactive $CD8^+$ Y-TILs ($P = 0.01$). Only few RCC tumor-reactive $CD8^+$ Y-TILs produced IFNγ compared with metastatic melanoma (less than 15% vs. almost 50%, $P = 0.002$; Fig. 3C). In contrast, more than 60% of RCC tumor-reactive $CD8^+$ T cells mobilized CD107a, and more than 40% mobilized CD107a as the only function, compared with less than 20% of tumor-reactive cells in metastatic melanoma ($P = 0.04$; Fig. 3D). TNF production was similar in RCC and metastatic melanoma (Fig. 3B); however, we also observed high TNF production in unstimulated samples (TILs without tumor), indicating that CD107a mobilization might be a more reliable marker for T-cell reactivity in populations with small responses in RCC. TNF production in representative unstimulated samples is shown in Figs. 2E and 3E and F. We therefore focused on the $CD8^+CD107a^+$ tumor-reactive T cells, and as indicated above, this population appeared less polyfunctional in RCC compared with in metastatic melanoma ($P = 0.07$; Supplementary Fig. S7A and S7B).

Dysfunctional profile of tumor-reactive $CD8^+$ TILs

Polyfunctionality and proliferative potential can be dependent on the differentiation status of T cells (34). Because of quite high TNF production in unstimulated samples (TILs without tumor) and because $CD8^+CD107a^+$ T cells appeared less polyfunctional in RCC compared with metastatic melanoma ($P = 0.07$; Supplementary Fig. S7A and S7B), we analyzed the differentiation/dysfunctional status of this tumor-reactive T-cell population. To this end, we analyzed the expression of PD-1, LAG-3, TIM-3, and CD57 on tumor-reactive $CD8^+$ Y-TILs from a smaller cohort of RCC and metastatic melanoma (8 patients in total). The relative distribution and combinatorial expression of these markers was similar in RCC and metastatic melanoma (Supplementary Fig. S8). Furthermore, we analyzed the expression of PD-1, LAG-3, TIM-3, and CD57 on unselected $CD8^+$ REP-TILs from an additional cohort of RCC and metastatic melanoma specimens as described in Materials and Methods (10 patients in total) and found similar results with no difference in the relative distribution of these markers in RCC and metastatic melanoma (Supplementary Fig. S9).

HLA class I expression and immune recognition of autologous TCLs

Polyfunctionality can be influenced by antigen presentation (33), and altered expression of the HLA class I antigen processing and presenting machinery (APM) is an immune escape mechanism in cancer (36). We have previously shown that autologous tumor recognition of metastatic melanoma TILs can be increased after pretreatment with low-dose IFNγ, which induce expression of the whole HLA class I APM (10). Therefore, we asked whether HLA class I downregulation could explain the lower magnitude and unique functional profile of $CD8^+$ T-cell responses observed in RCC compared with metastatic melanoma. We analyzed 12 RCC and 14 MM-TCLs and found HLA class I to be constitutively expressed in all samples, with a median MFI of HLA class I surface expression in RCC of 15.3 (range, 8.6–46.1) versus 12.5 (range, 5.4–25.5) in metastatic melanoma ($P = 0.25$; Supplementary Fig. S10). This was associated with a constitutive expression with major APM components. Although the expression of TAP2, tapasin, β_2-microglobulin (β_2m), and the HLA class I heavy chain (HC) was comparable, the TAP1 and LMP2 mRNA levels were expressed at higher level in RCC compared with metastatic melanoma (Supplementary Fig. S11). Pretreatment of TCLs with IFNγ increased HLA class I expression in both RCC and metastatic melanoma with a median MFI in RCC of 35.7 (range, 2.4–80.3) versus 28.6 (range, 7.2–48.5) in metastatic melanoma ($P = 0.63$; Supplementary Fig. S10). The IFNγ-mediated upregulation of HLA class I surface antigens was associated with an enhanced expression of all APM components analyzed with a similar induction level in both tumor types with the exception of TAP1 exhibiting only a 50% induction in RCC when compared with metastatic melanoma (Supplementary Figs. S12 and S13). This might be due to impaired constitutive but inducible TAP1 in metastatic melanoma. Next, we tested whether pretreatment of TCLs with IFNγ could improve tumor recognition. In RCC, immune recognition of $CD8^+$ T cells did not increase (Y-TILs, $P = 0.85$; REP-TILs, $P = 0.58$; Supplementary Figs. S14A and S14B). In metastatic melanoma, on the contrary, we have previously shown that responses can be increased after IFNγ exposure (10); however, in this small cohort, the increase in tumor responses after IFNγ exposure was not statistically significant ($P = 0.13$; Supplementary Fig. S14C). This difference in upregulation of tumor recognition between RCC and metastatic melanoma might be partly explained by constitutive TAP1 deficiencies in metastatic melanoma (which may lead to impaired tumor recognition, restored by IFNγ), but other, unknown factors may play a role as well.

In conclusion and in contrast to metastatic melanoma, these data suggested that a downregulation of HLA class I surface antigens due to impaired expression of APM components does not play a major role on $CD8^+$ T-cell–mediated recognition of RCC.

Tumor-reactive $CD4^+$ TILs

Tumor-specific $CD4^+$ T-cell responses may contribute to immunologic surveillance of cancers (37). In metastatic melanoma, $CD4^+$ TILs recognize naturally presented tumor antigens, including neoantigens, on MHC class II^+ cancer cells (11, 38). In RCC, $CD4^+$ T-cell responses against shared tumor antigens were previously detected in one patient (39). This prompted us to analyze whether $CD4^+$ RCC-TILs recognize autologous tumor antigens and how this compared with metastatic melanoma.

HLA class II was constitutively expressed, although at low levels, in only 2 of 12 RCC-TCLs (17%) tested. In comparison, 50% MM-TCLs tested (7/14) constitutively expressed HLA class II surface antigens, which is in line with previous literature (11, 40, 41; $P = 0.11$ vs. RCC; Supplementary Fig. S15A). As expected, almost all RCC (11/12) and metastatic melanoma (13/14) displayed HLA class II upregulation after treatment with IFNγ (Supplementary Fig. S15B).

$CD4^+$ T-cell responses against untreated autologous TCLs were observed in only 1 of 17 RCC (6%; RCC19 – HLA II status unknown) compared with 5/14 metastatic melanoma (36%; $P = 0.07$; Fig. 4A). Pretreatment of TCLs with IFNγ, which is known to upregulate HLA class II presentation, restored tumor recognition of $CD4^+$ Y-TILs in 5 additional patients with RCC

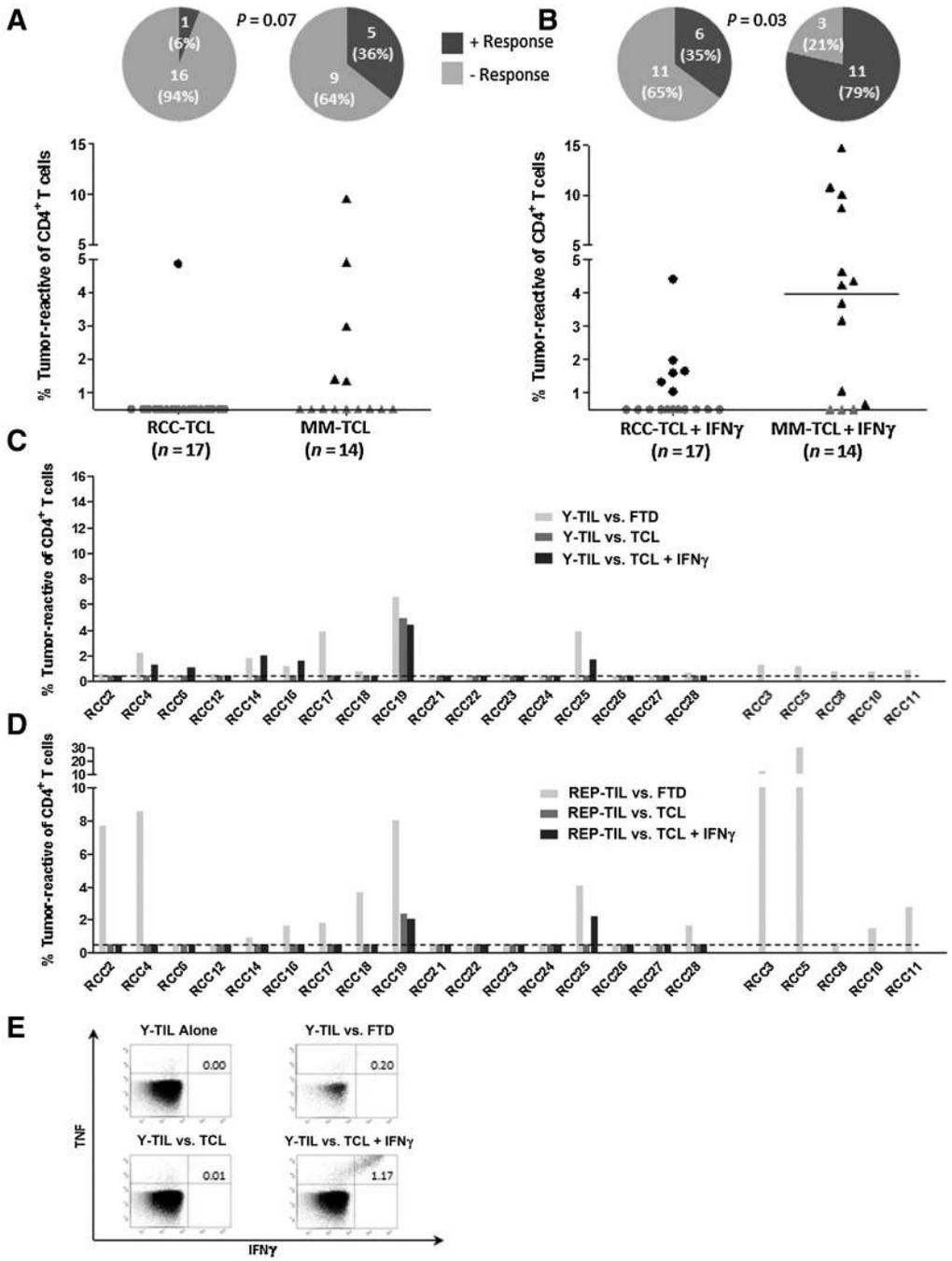

Figure 4.

$CD4^+$ T-cell responses in RCC and metastatic melanoma. The figure shows antitumor $CD4^+$ T-cell responses in RCC- ($n = 17$) and MM- ($n = 14$) Y-TILs and REP-TILs after coculture with autologous FTDs or TCLs, treated with IFNγ (TCL + IFNγ) or left untreated, as described in Materials and Methods. Tumor-reactive T cells are defined as T cells expressing at least one of the following T-cell functions: TNF, IFNγ, or CD107a. **A** and **B,** Top, the number/(%) of patients containing Y-TILs with (dark gray) or without (light gray) $CD4^+$ T-cell responses against TCLs ± IFNγ is shown in the pie charts. We found no statistically significant difference when comparing Y-TILs cocultured with untreated TCLs from RCC and metastatic melanoma ($P = 0.07$), whereas a higher percentage of MM-TILs had $CD4^+$ T-cell responses toward TCLs + IFNγ compared with RCC-TILs ($P = 0.03$). Bottom, dots and triangles represent RCC- and MM-TILs, respectively; black and gray symbols represent, respectively, Y-TILs with or without $CD4^+$ T-cell responses against TCLs ± IFNγ. Limit of detection was 0.5%. Lines, median values. The magnitude of $CD4^+$ T-cell responses in Y-TILs against autologous TCLs treated with IFNγ was not statistically significantly lower in RCC compared with metastatic melanoma (only TILs with responses are compared; $P = 0.08$). **C** and **D,** The percentages of tumor-reactive $CD4^+$ Y-TILs (**C**) and $CD4^+$ REP-TILs (**D**) after coculture with autologous FTDs (light gray bars), untreated TCLs (dark gray bars), or TCLs + IFNγ (black bars), in individual RCC patients, are shown. In patients where autologous TCLs were not available, TILs were only tested against FTDs (RCC3, RCC5, RCC8, RCC10, and RCC11). Dotted line, limit of detection (0.5%). **E,** The FACS plots demonstrate cytokine production from representative RCC-Y-TILs after coculture with autologous tumor cells.

(6/17, 35%; $P = 0.09$; Supplementary Fig. S16A). This is compared with a higher rate of responders in metastatic melanoma (11/14, 79%; $P = 0.03$ vs. RCC-Y-TILs; Fig. 4B; Supplementary Fig. S16B), although the frequency of responding patients with metastatic melanoma reported here appeared to be higher than previously reported by us in one larger cohort (11). The magnitude of $CD4^+$ T-cell responses in metastatic melanoma [in TILs with responses; median 4.4% (range, 0.7–14.7)] was not significantly stronger than in RCC [median, 1.6% (range 1.1–4.4); $P = 0.08$; Fig. 4B]. There were no differences in the frequency of $CD4^+$ T-cell responses in the RCC-REP-TIL population with or without IFNγ ($P = 0.6$; Supplementary Fig. S16C). $CD4^+$ T-cell responses to RCC-TCLs were only observed when tumor cells were either constitutively expressing HLA class II surface molecules or upon IFNγ treatment as previously shown in metastatic melanoma (10).

$CD4^+$ T-cell responses were detected against FTDs in 16 of 22 RCC-Y-TILs (73%) and 14 of 22 RCC-REP-TILs (64%), including 6 patients (RCC2, RCC12, RCC17, RCC18, RCC23, and RCC28), in which no CD4 T-cell reactivity against TCLs was found, neither in the absence or presence of IFNγ (Fig. 4C and D). FACS plots showing cytokine production (TNF and IFNγ) from $CD4^+$ RCC-Y-TILs after coculture with TCL are shown in a representative patient in Fig. 4E. FTDs may contain other stromal elements than solely tumor cells, including antigen-presenting cells (APC). Thus, in theory, $CD4^+$ T cells may recognize APCs presenting tumor-associated antigens that are not naturally processed and presented by tumor cells. For these reasons, we hypothesized that the actual frequency of $CD4^+$ T cells recognizing tumor-associated antigens may be higher than expected when using TCLs as targets.

Overall, $CD4^+$ T-cell responses in RCC-Y-TILs with direct recognition of naturally presented tumor antigens on TCLs appeared similar in frequency (77% vs. 77%, $P = 1$) but slightly lower in magnitude [median 1.05 (range, 0.52–6.6) vs. median 1.6 (range, 0.6–14.2), $P = 0.11$] compared with $CD8^+$ T-cell responses. In the whole cohort, we found only 3 patients with RCC (3/22, 14%) with no detectable $CD4^+$ and/or $CD8^+$ T-cell responses, suggesting that tumor-specific T-cell responses occur in the majority of RCC patients (19/22, 86%).

Discussion

The presence of tumor-reactive T cells in the microenvironment of cancers appears a prerequisite for the efficacy of PD-1–blocking agents (42) and adoptive transfer with autologous TILs, which is based on TIL isolation and expansion. High expression of immune activation markers *in situ* (43–45) and depletion of immunogenic neoepitopes (43) suggested that the TME of primary RCCs might harbor tumor-specific T cells with immunosurveillance functions. In comparison, other highly immunogenic tumors, such as metastatic melanoma, where current immunotherapies with PD-1/PD-L1 inhibitors has so far shown the highest response rates (46), displayed only average immune activation at the tumor site (43), in spite of a higher mutational burden (47). A high proportion and number of indels in RCC tumors providing high-affinity neoepitope may explain the high rate of T-cell activation and clinical responses to PD-1 checkpoint inhibitors in this tumor type (48).

In this study, metastatic melanoma was chosen as reference comparison primarily because the infusion of autologous TILs could cure patients with widely metastatic disease in several independent studies (1, 4, 6, 8). Minimally expanded TILs from metastatic melanoma contain large fractions of $CD8^+$ and $CD4^+$ tumor-reactive T cells, which recognize different types of antigens, including mutant neoantigens (38, 49). Therefore, the ability to manufacture TILs with similar features of those observed in metastatic melanoma warrants testing of TIL immunotherapy in other tumors. Here, we showed that naturally occurring tumor-reactive T cells can be detected, recovered, and expanded *in vitro* from a large fraction of RCC patients. Despite some differences, such as CD4/CD8 ratio, the phenotype of TILs recovered from RCCs appeared similar to MM-TILs. Tumor-reactive T cells were recovered from the TME in 86% of RCCs, with over 50% of specimens bearing tumor-reactive $CD4^+$ T cells, which in many cases could directly recognize tumor cells. However, in comparison with TILs from metastatic melanoma, antitumor responses appeared weaker with typically only a few percent of T cells able to recognize autologous tumor antigens. Other studies have analyzed the phenotype and function of TILs in nonmelanoma solid tumor histologies. The analysis of TIL phenotype showed similar results in most studies published to date, with the majority of expanded cells expressing markers consistent with antigen-experienced effector memory cells (15, 50). In five recent studies from the NCI, Surgery Branch (Bethesda, MD), TILs from gastrointestinal cancers were characterized (15, 51–54). In two clinical cases, infusion of TILs recognizing mutant antigens induced tumor regression (53, 54). Nevertheless, although tumors from the majority of patients contained tumor-reactive T cells (15, 51), the frequency of unselected tumor-reactive TILs reported in these studies was low (0%–3%) compared with metastatic melanoma (15). In another study from the same group, Stevanovic and colleagues (16) treated 9 patients with cervical cancer with autologous TILs. Clinical responses were observed in 3 patients treated with TILs with high HPV reactivity. TIL reactivity was demonstrated in 6 of 9 patients (66%) with a CD137 upregulation assay, but it appeared that 3 patients without clinical responses had low *in vitro* reactivity. Preliminary results in head and neck (55) as well as ovarian cancer (56) sarcoma (57) and uveal melanoma (58) demonstrated that tumor-reactive TILs could be recovered from the TME of all these types of tumors. Overall, it appears that tumor-reactive TILs can be recovered from most tumor types studied. However, the magnitudes of responses appear lower than in metastatic melanoma and can vary between individual patients. Taken together, these data warrant further development of methods for enrichment, including selection of TIL microcultures with particularly high antigen reactivity (53, 54), sorting based on activation markers upon antigen recognition (59), or streptamer-based enrichment (60). However, in this study, we also show that classical REP with IL2 or combinations of IL7, IL15, and IL21 does not efficiently support the expansion of tumor-reactive TILs from RCC. A dysfunctional profile of tumor-reactive TILs did not appear to be associated with a lower proliferative potential. Thus, further studies should explore other ways to expand massively tumor-reactive TILs from RCC.

Polyfunctionality is a desirable feature of potent $CD8^+$ T cells that is often found in infections (29), but described less frequently in cancer immunity (11, 30). Tumor-reactive $CD8^+$ T cells in

RCC were less polyfunctional compared with their metastatic melanoma counterpart and especially produced less IFNγ. These data may explain the discrepancy previously observed by Markel and colleagues (12), who reported data on six pairs of TILs and autologous RCC lines with cytotoxicity without IFNγ production in 3 of 6 patients analyzed. In our study, lower polyfunctionality compared with metastatic melanoma did not appear to associate to a more exhausted profile of tumor-reactive $CD8^+$ T cells. However, polyfunctionality may be a function of the intensity of stimulation of the TCR, influenced by the densities of HLA class I antigen complexes on the target cells and antigen sensitivity of the effector T cell (33, 61). According to data obtained with virus-specific $CD8^+$ T cells, CD107a mobilization is influenced to a minor extent by antigen concentration compared with IFNγ, and this may explain why RCC-specific $CD8^+$ T cells mobilized CD107a but did not produce IFNγ. Because we could not identify target antigens in RCC, we were not able to determine whether the RCC tumor–reactive TILs had lower antigen sensitivity, or their cognate antigens were expressed at lower levels on target cells. However, RCC cell lines exhibit comparable constitutive and IFNγ-inducible expression levels of major APM components and HLA class I surface molecules when compared with metastatic melanoma. In contrast to metastatic melanoma, global tumor recognition of RCC-TCLs was not increased upon preexposure to IFNγ despite increase of HLA class I surface antigens. Thus, universal downregulation of HLA class I antigens did not appear to be a major issue in RCC and is unlikely to be responsible for the mono/oligofunctional responses observed. Further studies to determine whether primary functional deficiencies of RCC tumor–reactive $CD8^+$ TILs may induce this unique functional profile are ongoing at our laboratory. Nonetheless, these findings provide guidance for immuno-monitoring studies in RCC where IFNγ assays (e.g., IFNγ ELISPOT or ELISA, which are commonly used for this purpose) might not detect otherwise tumor-reactive $CD8^+$ T cells.

The role of tumor-reactive $CD4^+$ TILs in cancer is currently a matter of debate. In metastatic melanoma, it was demonstrated that the TME of most patients contains $CD4^+$ TILs, which can recognize tumor antigens, including products of cancer mutations, presented directly from tumor cells in association with HLA class II (11, 38, 62). Direct infusion of $CD4^+$ T cells enriched for recognition of one mutant antigen mediated tumor regression of a gastrointestinal cancer (53). However, the beneficial role of tumor-reactive $CD4^+$ T cells in metastatic melanoma was recently questioned by our group through the demonstration of a monofunctional pattern in most effector cells (11). Fifty percent of metastatic melanomas express constitutively HLA class II molecules (11, 40), and this is known to associate with stronger tumor-specific $CD4^+$ T-cell responses (11). In this study, only 2 of 12 RCCs (17%) expressed HLA class II constitutively, but upregulation of HLA class II molecules with cytokines revealed $CD4^+$ tumor recognition in over 50% of patients. These data demonstrate that generation of tumor-specific $CD4^+$ T cells is a frequent event in primary RCC, but therapeutic exploitation of direct $CD4^+$ T-cell responses will require upregulation of HLA class II molecules by other means, such as cotransfer of tumor-reactive $CD8^+$ T cells to produce IFNγ in the TME.

This study suffers from two intrinsic drawbacks. First, the samples used in this study were obtained from primary RCCs, which were compared with metastases of melanoma. Second, RCC lesions are known to have high inter- and intratumor heterogeneity (20, 63). However, a study characterizing the TME and its prognostic relevance in primary versus metastatic clear cell RCC found a comparable immune cell infiltration pattern in primary to metastatic tumors (64). Third, RCCs are generally highly vascularized tumors, which increases the risk for contamination of TIL cultures with PBLs, thereby diluting tumor-reactive cells. This might contribute to the low tumor responses observed, but does not explain the differences in functionality of $CD8^+$ tumor-reactive TILs. If RCC lesions will be used for the generation of clinical grade TILs, one would have to be careful to not contaminate TIL cultures with PBLs, and thus diluting tumor-reactive cells in the TIL product.

In conclusion, TILs from RCC can be expanded to clinical relevant numbers using the Y-TIL expansion methods, and TILs obtained from most patients contain tumor-reactive $CD4^+$ and $CD8^+$ T cells. However, immune responses of expanded TILs from RCC are on average weaker and less polyfunctional than observed in metastatic melanoma. The ability to select, enrich, and expand tumor-reactive polyfunctional T cells may be critical in developing effective ACT with autologous TILs for RCC.

Disclosure of Potential Conflicts of Interest

No potential conflicts of interest were disclosed.

Authors' Contributions

Conception and design: R. Andersen, B. Seliger, M. Donia, I.M. Svane
Development of methodology: R. Andersen, S.R. Hadrup, M. Donia
Acquisition of data (provided animals, acquired and managed patients, provided facilities, etc.): R. Andersen, M.C.W. Westergaard, N.W. Pedersen, B. Seliger, B. Kromann-Andersen, I.M. Svane
Analysis and interpretation of data (e.g., statistical analysis, biostatistics, computational analysis): R. Andersen, M.C.W. Westergaard, J.W. Kjeldsen, A. Müller, N.W. Pedersen, S.R. Hadrup, Ö. Met, B. Seliger, B. Kromann-Andersen, M. Donia
Writing, review, and/or revision of the manuscript: R. Andersen, M.C.W. Westergaard, J.W. Kjeldsen, Ö. Met, B. Seliger, B. Kromann-Andersen, M. Donia, I.M. Svane
Administrative, technical, or material support (i.e., reporting or organizing data, constructing databases): R. Andersen, M.C.W. Westergaard, J.W. Kjeldsen, T. Hasselager, I.M. Svane
Study supervision: R. Andersen, B. Seliger, B. Kromann-Andersen, M. Donia, I.M. Svane

Acknowledgments

The studies were supported by grants from the Research Council from Herlev Hospital, The Danish Cancer Society, The Danish Cancer Research Foundation, and the Mildred Scheel Cancer Aid Foundation (B. Seliger) grant 110703 and 111091.

Lisbeth Egelykke Stolpe, Sandra Ullitz Færch, and Susanne Wendt are acknowledged for technical assistance. Lillian Føns is acknowledged for assistance in patient inclusion.

The costs of publication of this article were defrayed in part by the payment of page charges. This article must therefore be hereby marked *advertisement* in accordance with 18 U.S.C. Section 1734 solely to indicate this fact.

Received August 25, 2017; revised December 8, 2017; accepted December 18, 2017; published OnlineFirst January 4, 2018.

References

1. Rosenberg SA, Yang JC, Sherry RM, Kammula US, Hughes MS, Phan GQ, et al. Durable complete responses in heavily pretreated patients with metastatic melanoma using T-cell transfer immunotherapy. Clin Cancer Res 2011;17:4550–7.
2. Dudley ME, Yang JC, Sherry R, Hughes MS, Royal R, Kammula U, et al. Adoptive cell therapy for patients with metastatic melanoma: evaluation of intensive myeloablative chemoradiation preparative regimens. J Clin Oncol 2008;26:5233–9.
3. Besser MJ, Shapira-Frommer R, Treves AJ, Zippel D, Itzhaki O, Hershkovitz L, et al. Clinical responses in a phase II study using adoptive transfer of short-term cultured tumor infiltration lymphocytes in metastatic melanoma patients. Clin Cancer Res 2010;16:2646–55.
4. Besser MJ, Shapira-Frommer R, Itzhaki O, Treves AJ, Zippel DB, Levy D, et al. Adoptive transfer of tumor-infiltrating lymphocytes in patients with metastatic melanoma: intent-to-treat analysis and efficacy after failure to prior immunotherapies. Clin cancer Res 2013;19:4792–800.
5. Pilon-Thomas S, Kuhn L, Ellwanger S, Janssen W, Royster E, Marzban S, et al. Efficacy of adoptive cell transfer of tumor-infiltrating lymphocytes after lymphopenia induction for metastatic melanoma. J Immunother 2012;35:615–20.
6. Radvanyi LG, Bernatchez C, Zhang M, Fox PS, Miller P, Chacon J, et al. Specific lymphocyte subsets predict response to adoptive cell therapy using expanded autologous tumor-infiltrating lymphocytes in metastatic melanoma patients. Clin Cancer Res 2012;18:6758–70.
7. Ellebaek E, Iversen TZ, Junker N, Donia M, Engell-Noerregaard L, Met O, et al. Adoptive cell therapy with autologous tumor infiltrating lymphocytes and low-dose Interleukin-2 in metastatic melanoma patients. J Transl Med 2012;10:169.
8. Andersen R, Donia M, Ellebæk E, Borch TH, Kongsted P, Iversen TZ, et al. Long-lasting complete responses in patients with metastatic melanoma after adoptive cell therapy with tumor-infiltrating lymphocytes and an attenuated IL-2 regimen. Clin Cancer Res 2016;22:3734–45.
9. Hinrichs CS, Rosenberg SA. Exploiting the curative potential of adoptive T-cell therapy for cancer. Immunol Rev 2014;257:56–71.
10. Donia M, Hansen M, Sendrup SL, Iversen TZ, Ellebæk E, Andersen MH, et al. Methods to improve adoptive T-cell therapy for melanoma: IFN-γ enhances anticancer responses of cell products for infusion. J Invest Dermatol 2012;133:545–52.
11. Donia M, Andersen R, Kjeldsen JW, Fagone P, Munir S, Nicoletti F, et al. Aberrant expression of MHC class II in melanoma attracts inflammatory tumor specific CD4+ T cells which dampen CD8+ T cell antitumor reactivity. Cancer Res 2015;75:3747–60.
12. Markel G, Cohen-Sinai T, Besser MJ, Oved K, Itzhaki O, Seidman R, et al. Preclinical evaluation of adoptive cell therapy for patients with metastatic renal cell carcinoma. Anticancer Res 2009;29:145–54.
13. Wang QJ, Hanada K-I, Robbins PF, Li YF, Yang JC. Distinctive features of the differentiated phenotype and infiltration of tumor-reactive lymphocytes in clear cell renal cell carcinoma. Cancer Res 2012;72:6119–29.
14. Baldan V, Griffiths R, Hawkins RE, Gilham DE. Efficient and reproducible generation of tumour-infiltrating lymphocytes for renal cell carcinoma. Br J Cancer 2015;112:1510–8.
15. Turcotte S, Gros A, Hogan K, Tran E, Hinrichs CS, Wunderlich JR, et al. Phenotype and function of T cells infiltrating visceral metastases from gastrointestinal cancers and melanoma: implications for adoptive cell transfer therapy. J Immunol 2013;191:2217–25.
16. Stevanović S, Draper LM, Langhan MM, Campbell TE, Kwong ML, Wunderlich JR, et al. Complete regression of metastatic cervical cancer after treatment with human papillomavirus-targeted tumor-infiltrating T cells. J Clin Oncol 2015;33:1543–50.
17. Andersen R, Donia M, Westergaard MCW, Pedersen M, Hansen M, Svane IM. Tumor infiltrating lymphocyte therapy for ovarian cancer and renal cell carcinoma. Hum Vaccin Immunother 2015;11:2790–5.
18. Fyfe G, Fisher RI, Rosenberg SA, Sznol M, Parkinson DR, Louie AC. Results of treatment of 255 patients with metastatic renal cell carcinoma who received high-dose recombinant interleukin-2 therapy. J Clin Oncol 1995;13:688–96.
19. Motzer RJ, Escudier B, McDermott DF, George S, Hammers HJ, Srinivas S, et al. Nivolumab versus everolimus in advanced renal-cell carcinoma. N Engl J Med 2015;373:1803–13.
20. Gerlinger M, Rowan AJ, Horswell S, Larkin J, Endesfelder D, Gronroos E, et al. Intratumor heterogeneity and branched evolution revealed by multiregion sequencing. N Engl J Med 2012;366:883–92.
21. Donia M, Junker N, Ellebaek E, Andersen MH, Straten PT, Svane IM. Characterization and comparison of "Standard" and "Young" tumor infiltrating lymphocytes for adoptive cell therapy at a Danish Translational Research Institution. Scand J Immunol 2012;75:157–67.
22. Fischer AH, Zhao C, Li QK, Gustafson KS, Eltoum I-EE, Tambouret R, et al. The cytologic criteria of malignancy. J Cell Biochem 2010;110:795–811.
23. Andersen MH, Bonfill JE, Neisig A, Arsequell G, Sondergaard I, Valencia G, et al. Phosphorylated peptides can be transported by TAP molecules, presented by class I MHC molecules, and recognized by phosphopeptide-specific CTL. J Immunol 1999;163:3812–8.
24. Steven A, Leisz S, Massa C, Iezzi M, Lattanzio R, Lamolinara A, et al. HER-2/neu mediates oncogenic transformation via altered CREB expression and function. Mol Cancer Res 2013;11:1462–77.
25. Roederer M, Nozzi JL, Nason MC. SPICE: exploration and analysis of post-cytometric complex multivariate datasets. Cytometry A 2011;79:167–74.
26. Kvistborg P, Shu CJ, Heemskerk B, Fankhauser M, Thrue CA, Toebes M, et al. TIL therapy broadens the tumor-reactive CD8+ T cell compartment in melanoma patients. Oncoimmunology 2012;1:409–18.
27. Ye Q, Song D-G, Poussin M, Yamamoto T, Best A, Li C, et al. CD137 accurately identifies and enriches for naturally occurring tumor-reactive T cells in tumor. Clin Cancer Res 2014;20:44–55.
28. Li Y, Liu S, Hernandez J, Vence L, Hwu P, Radvanyi L. MART-1-specific melanoma tumor-infiltrating lymphocytes maintaining CD28 expression have improved survival and expansion capability following antigenic restimulation *in vitro*. J Immunol 2010;184:452–65.
29. Seder RA, Darrah PA, Roederer M. T-cell quality in memory and protection: implications for vaccine design. Nat Rev Immunol 2008;8:247–58.
30. Berinstein NL, Karkada M, Oza AM, Odunsi K, Villella JA, Nemunaitis JJ, et al. Survivin-targeted immunotherapy drives robust polyfunctional T cell generation and differentiation in advanced ovarian cancer patients. Oncoimmunology 2015;4:e1026529.
31. Tan MP, Gerry AB, Brewer JE, Melchiori L, Bridgeman JS, Bennett AD, et al. T cell receptor binding affinity governs the functional profile of cancer-specific CD8+ T cells. Clin Exp Immunol 2015;180:255–70.
32. Tan MP, Dolton GM, Gerry AB, Brewer JE, Bennett AD, Pumphrey NJ, et al. Human leucocyte antigen class I-redirected anti-tumour CD4 $^{+}$ T cells require a higher T cell receptor binding affinity for optimal activity than CD8 $^{+}$ T cells. Clin Exp Immunol 2017;187:124–37.
33. Almeida J, Sauce D, Price D, Papagno L, Shin S, Moris A, et al. Antigen sensitivity is a major determinant of CD8+ T-cell polyfunctionality and HIV suppressive activity. Blood 2009;113:6351–60.
34. Karagiannis P, Iriguchi S, Kaneko S. Reprogramming away from the exhausted T cell state. Semin Immunol 2016;28:35–44.
35. Donia M, Kjeldsen JW, Andersen R, Wulff MC, Bianchi V, Legut M, et al. PD-1+ polyfunctional T cells dominate the periphery after tumor-infiltrating lymphocyte therapy for cancer. Clin Cancer Res 2017;23:5779–88.
36. del Campo A, Carretero J, Aptsiauri N, Garrido F. Targeting HLA class I expression to increase tumor immunogenicity. Tissue Antigens 2012;79:147–54.
37. Hadrup S, Donia M, Thor Straten P. Effector CD4 and CD8 T cells and their role in the tumor microenvironment. Cancer Microenviron 2012;6:123–33.
38. Linnemann C, van Buuren MM, Bies L, Verdegaal EM, Schotte R, Calis JJ, et al. High-throughput epitope discovery reveals frequent recognition of neo-antigens by CD4+ T cells in human melanoma. Nat Med 2015;21:81–5.
39. Mautner J, Jaffee EM, Pardoll DM. Tumor-specific CD4+ T cells from a patient with renal cell carcinoma recognize diverse shared antigens. Int J Cancer 2005;115:752–9.
40. Mendez R, Aptsiauri N, Del Campo A, Maleno I, Cabrera T, Ruiz-Cabello F, et al. HLA and melanoma: multiple alterations in HLA class I and II expression in human melanoma cell lines from ESTDAB cell bank. Cancer Immunol Immunother 2009;58:1507–15.
41. Seliger B, Kloor M, Ferrone S. HLA class II antigen-processing pathway in tumors: molecular defects and clinical relevance. Oncoimmunology 2017;6:e1171447.

42. Tumeh PC, Harview CL, Yearley JH, Shintaku IP, Taylor EJ, Robert L, et al. PD-1 blockade induces responses by inhibiting adaptive immune resistance. Nature 2014;515:568–71.
43. Rooney MS, Shukla SA, Wu CJ, Getz G, Hacohen N. Molecular and genetic properties of tumors associated with local immune cytolytic activity. Cell 2015;160:48–61.
44. Spranger S, Luke JJ, Bao R, Zha Y, Hernandez KM, Li Y, et al. Density of immunogenic antigens does not explain the presence or absence of the T-cell–inflamed tumor microenvironment in melanoma. Proc Natl Acad Sci U S A 2016;113:E7759–68.
45. Senbabaoglu Y, Gejman RS, Winer AG, Liu M, Van Allen EM. Tumor immune microenvironment characterization in clear cell renal cell carcinoma identifies prognostic and immunotherapeutically relevant messenger RNA signatures. Genome Biol 2016;17:231.
46. Borch TH, Donia M, Andersen MH, Svane IM. Reorienting the immune system in the treatment of cancer by using anti-PD-1 and anti-PD-L1 antibodies. Drug Discov Today 2015;20:1127–34.
47. Alexandrov LB, Nik-Zainal S, Wedge DC, Aparicio SA Jr, Behjati S, Biankin AV, et al. Signatures of mutational processes in human cancer. Nature 2013;500:415–21.
48. Turajlic S, Litchfield K, Xu H, Rosenthal R, McGranahan N, Reading JL, et al. Insertion-and-deletion-derived tumour-specific neoantigens and the immunogenic phenotype: a pan-cancer analysis. Lancet Oncol 2017;18:1009–21.
49. Robbins PF, Lu YC, El-Gamil M, Li YF, Gross C, Gartner J, et al. Mining exomic sequencing data to identify mutated antigens recognized by adoptively transferred tumor-reactive T cells. Nat Med 2013;19:747–52.
50. Chandran SS, Paria BC, Srivastava AK, Rotherme LD, Stephens DJ, Kammula US, et al. Tumor-specific effector CD8+ T cells that can establish immunological memory in humans after adoptive transfer are marked by expression of IL7 receptor and c-myc. Cancer Res 2015;75:3216–26.
51. Turcotte S, Gros A, Tran E, Lee CC, Wunderlich JR, Robbins PF, et al. Tumor-Reactive CD8+ T cells in metastatic gastrointestinal cancer refractory to chemotherapy. Clin Cancer Res 2014;20:331–43.
52. Tran E, Ahmadzadeh M, Lu Y, Gros A, Turcotte S, Robbins PF, et al. Immunogenicity of somatic mutations in human gastrointestinal cancers. Science 2015;350:1387–90.
53. Tran E, Turcotte S, Gros A, Robbins P. Cancer immunotherapy based on mutation-specific CD4+ T cells in a patient with epithelial cancer. Science 2014;9:641–6.
54. Tran E, Robbins PF, Lu YC, Prickett TD, Gartner JJ, Jia L, et al. T-cell transfer therapy targeting mutant KRAS in cancer. N Engl J Med 2016; 375:2255–62.
55. Junker N, Andersen MH, Wenandy L, Dombernowsky SL, Kiss K, Sørensen CH, et al. Bimodal ex vivo expansion of T cells from patients with head and neck squamous cell carcinoma: a prerequisite for adoptive cell transfer. Cytotherapy 2011;13:822–34.
56. Westergaard MCW, Andersen R, Kjeldsen JW, Hasselager T, Lajer H, Donia M, et al. Preclinical development of tumor-infiltrating lymphocytes (TILs) based adoptive cell transfer immunotherapy (ACT) for patients with advanced ovarian cancer. Ann Oncol 2016;27:8s, 2016 (suppl).
57. Nielsen M, Krarup-Hansen A, Hovgaard D, Petersen MM, Loya AC, Junker N, et al. Expansion of tumor specific tumor infiltrating lymphocytes (TIL) from sarcoma and the potential benefit of anti-CD137 stimulation: a prerequisite for adoptive cell transfer (ACT) immunotherapy. In: ESMO Immuno-Oncology Congress 2017; 2017 Dec 7–10; Geneva, Switzerland. Ann Oncol 28:11s, 2017 (suppl).
58. Rothermel LD, Sabesan AC, Stephens DJ, Chandran SS, Paria BC, Srivastava AK, et al. Identification of an immunogenic subset of metastatic uveal melanoma. Clin Cancer Res 2016;22:2237–49.
59. Rosenberg SA, Restifo NP. Adoptive cell transfer as personalized immunotherapy for human cancer. Science 2015;348:62–8.
60. Kelderman S, Heemskerk B, Fanchi L, Philips D, Toebes M, Kvistborg P, et al. Antigen-specific TIL therapy for melanoma: a flexible platform for personalized cancer immunotherapy. Eur J Immunol 2016; 46:1351–60.
61. Chiu YL, Shan L, Huang H, Haupt C, Bessell C, Canaday DH, et al. Sprouty-2 regulates HIV-specific T cell polyfunctionality. J Clin Invest 2014;124: 198–208.
62. Friedman KM, Prieto PA, Devillier LE, Gross CA, Yang JC, Wunderlich JR, et al. Tumor-specific CD4+ melanoma tumor-infiltrating lymphocytes. J Immunother 2012;35:400–8.
63. Fisher R, Larkin J, Swanton C. Inter and intratumour heterogeneity: a barrier to individualized medical therapy in renal cell carcinoma? Front Oncol 2012;2:49.
64. Remark R, Alifano M, Cremer I, Lupo A, Dieu-Nosjean MC, Riquet M, et al. Characteristics and clinical impacts of the immune environments in colorectal and renal cell carcinoma lung metastases: influence of tumor origin. Clin Cancer Res 2013;19:4079–91.